# CHARACTERIZATION OF CARAMEL JAM USING BACK EXTRUSION TECHNIQUE

E[1].*CASTRO, C.° SILVA, F.# OSORIO and M.*MIRANDA.

** Departamento de Ciencia de los Alimentos y Tecnología Química, Universidad de Chile. Santiago, Chile.*

*° Ingeniero en Alimentos*

*# Departamento de Ciencia y Tecnología de los Alimentos, Universidad de Santiago de Chile. Santiago, Chile.*

**Keywords**: Back extrusion, caramel jam, Bingham, Power law

**Abstract:**

**Back extrusion technique was applied to characterize caramel jam samples taken from Chilean market. Determinations were made at room temperature, working with a Lloyd Universal material testing machine model LR 5K with a 500 N cell.**

**Power law and Bingham plastic models were applied.**

**Calculations were made with a spreadsheet (QPRO), and statistical analyses were done using a statistical package (STATGRAPHICS).**

**Results indicated that the Bingham plastic model showed the best goodness of fit, and that an increase in soluble solid content caused an increase in yield stress.**

## 1. Introduction

Rheological characterization is very important for textural determination, food stability and process design. Instruments used for rheological characterization of food are based on the mechanical operation over the sample and give results based on strength, strain or time (deMan *et al*., 1976). Back extrusion testing, sometimes called annular pumping, has a great potential for the food industry as a quality control tool, and as mean of determining rheological properties required to solve various engineering design problems (Osorio and Steffe, 1987).

Back extrusion testing requires simple equipment such as plunger, cylindrical container and a Universal Material Testing Machine (Osorio and Steffe, 1987). This is an easy and reliable technique to determine rheological properties and to make the technique a good candidate for quality control and product development work.

The objectives of this study were to characterize chilean caramel jam using back extrusion technique.

### 1.1 Back extrusion

In this methodology a cylindrical plunger is traveling vertically at a constant velocity, forced down into a fluid in a cylindrical container; the moving plunger volumetrically displaces the fluid, causing it to flow upwards through the annular space between the plunger and inner wall of the cylindrical container, Fig. 1 depicts a typical position of the plunger before and after back extrusion test (Osorio and Steffe, 1987).

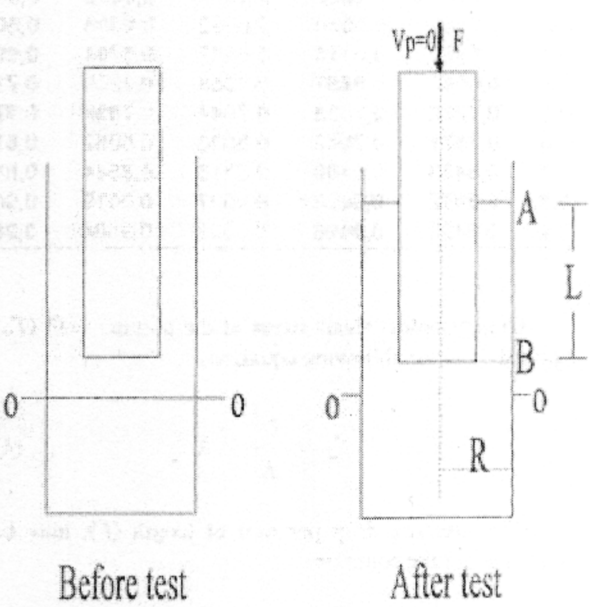


Figure 1. Schematic representation of plunger position before and after extrusion test.

The following assumptions were made: constant temperature and density, homogenous fluid, no elasticity or time dependent behavior, laminar and fully developed flow, the cylinder is sufficiently long that ends effects may be neglected, no slip at the walls of the annulus.

At a constant plunger velocity, the total force

[1] Author to whom correspondence should be addressed

applied to the plunger is equal to the force due to the shear stress on the plunger wall plus the force due to the static pressure pushing upward on the bottom surface of the plunger.

The axial flow of a power law fluid is analyzed in annular space.

1.2 Ostwald-de-Waele model

A power law fluid is tested in a back extrusion device at two different plunger velocities with the same plunger and cylinder, and it is possible to determine the flow behavior index defined by the following equation (Osorio and Steffe, 1985).

$$n = \frac{ln\left(\frac{F_{cb_2} L_1}{F_{cb_1} L_2}\right)}{ln\left(\frac{V_{p_2}}{V_{p_1}}\right)} \quad (1)$$

The flow behavior index, n, is the slope of a log-log plot of $(F_{cb_2} / F_{cb_1})(L_1 / L_2)$ against $(V_{p_2} / V_{p_1})$ (Osorio and Steffe, 1987).

The force corrected by buoyancy is (Osorio and Steffe, 1985):

$$F_{cb} = F_T - F_b \quad (2)$$

$$F_b = dgL\,\pi a^2 \quad (3)$$

For a power law fluid, the buoyancy force is the recorded force after the plunger is stopped ($F_{T*}$) and this value is experimentally obtained (See Fig. 4).

$K$ is calculated from $K = a/R$. $\lambda$ value can be obtained from Table 1 knowing the flow behavior index (n) and the system geometry $K$.

Table 1. Values for different values of $K$ and n

| K/n | 0,1 | 0,2 | 0,3 | 0,4 | 0,5 | 0,6 | 0,7 | 0,8 | 0,9 | 1,0 |
|---|---|---|---|---|---|---|---|---|---|---|
| 0,1 | 0,4065 | 0,4889 | 0,5539 | 0,6009 | 0,6344 | 0,6586 | 0,6768 | 0,6907 | 0,7017 | 0,7106 |
| 0,2 | 0,5140 | 0,5680 | 0,6092 | 0,6398 | 0,6628 | 0,6803 | 0,6940 | 0,7049 | 0,7138 | 0,7211 |
| 0,3 | 0,5951 | 0,6313 | 0,6587 | 0,6794 | 0,6953 | 0,7078 | 0,7177 | 0,7259 | 0,7326 | 0,7382 |
| 0,4 | 0,6647 | 0,6887 | 0,7068 | 0,7206 | 0,7313 | 0,7399 | 0,7469 | 0,7527 | 0,7575 | 0,7616 |
| 0,5 | 0,7280 | 0,7433 | 0,7547 | 0,7636 | 0,7705 | 0,7761 | 0,7807 | 0,7846 | 0,7878 | 0,7906 |
| 0,6 | 0,7871 | 0,7962 | 0,8030 | 0,8082 | 0,8124 | 0,8158 | 0,8186 | 0,8209 | 0,8229 | 0,8246 |
| 0,7 | 0,8433 | 0,8480 | 0,8516 | 0,8544 | 0,8566 | 0,8584 | 0,8599 | 0,8611 | 0,8622 | 0,8631 |
| 0,8 | 0,8972 | 0,8992 | 0,9007 | 0,9019 | 0,9028 | 0,9035 | 0,9042 | 0,9047 | 0,9052 | 0,9055 |
| 0,9 | 0,9493 | 0,9498 | 0,9502 | 0,9504 | 0,9507 | 0,9508 | 0,9510 | 0,9511 | 0,9512 | 0,9513 |

(Osorio, 1985)

Dimensionless shear stress at the plunger wall ($T_w$) is obtained from the following equation:

$$T_w = \frac{\lambda^2}{K} - K \quad (4)$$

The pressure drop per unit of length ($P$), may be calculated using the equation:

$$P = \frac{F_{cb}}{(T_w + K)\pi LRa} \quad (5)$$

The shear stress ($\sigma$) is obtained as (Osorio y Steffe, 1985):

$$\sigma = \frac{PRT_w}{2} \quad (6)$$

The dimensionless flow rate values for a selected set of $K$ and n values are presented in Fig. 2.

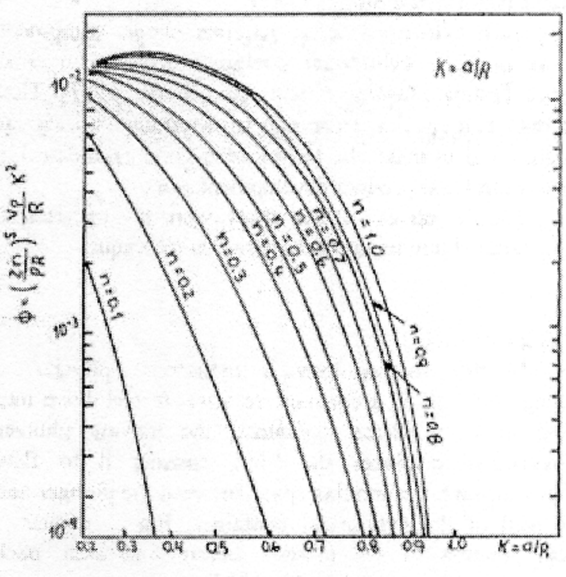


Figure 2. Dimensionless flow rate versus dimensionless plunger radius as a function of the flow behavior index for back extrusion of a power law fluid (Osorio, 1985).

The consistency coefficient ($\eta$) is obtained as (Osorio and Steffe, 1985):

$$\eta = \frac{PR}{2}\left(\frac{\Phi R}{V_p K^2}\right)^n \tag{7}$$

Then, shear rate ($\dot{\gamma}$) is obtained as (Osorio and Steffe, 1985):

$$\dot{\gamma} = \left(\frac{PR}{2\eta}\right)^{1/n} \left.\frac{d\phi}{d\rho}\right|_{\rho = K} \tag{8}$$

For power law fluid, the dimensionless shear rate is obtained with the $\lambda$ value as:

$$\left.\frac{d\phi}{d\rho}\right|_{\rho = K} = \left(\frac{\lambda^2}{K} - K\right)^{1/n} \tag{9}$$

1.3 Bingham plastic model

The first step in the calculations is to determine the yield stress as:

$$\sigma_0 = \frac{F_{T_s} - F_b}{2\pi a L} \tag{10}$$

$F_{T_s}$ is determined experimentally (See Fig. 4).

The plastic viscosity ($\eta_p$) is determined by iteration. A dimensionless yield stress ($T_0$) is assumed and the pressure drop per unit of length ($P$) is determined as:

$$P = \frac{2\sigma_0}{T_0 R}, \tag{11}$$

With $T_0$ and $K$ values determine $\Phi$ using Fig. 3 for n = 1. The $\lambda$ values for different values of $K$ and $T_0$ are shown in Table 2.

Dimensionless yield stress at the plunger wall ($T_w$) is obtained as (Osorio, 1985):

$$T_w = \frac{\lambda(\lambda - T_0)}{K} - K \tag{12}$$

And the plastic viscosity is obtained as:

$$\eta_p = \frac{\Phi P R^2}{2 V_p K^2} \tag{13}$$

The $\Phi$ value is obtained from Figure 3.

The following step is to compute the expression $P(T_w + K)$. If the calculated value is equal to $(F_{eb}/\pi L R a)$, then $T_0$ value is correct and the iteration stops; the $\eta_p$ values, then the following equation is used:

$$\dot{\gamma} = \frac{PR}{2\eta_p} \left.\frac{d\phi}{d\rho}\right|_{\rho = K} \tag{14}$$

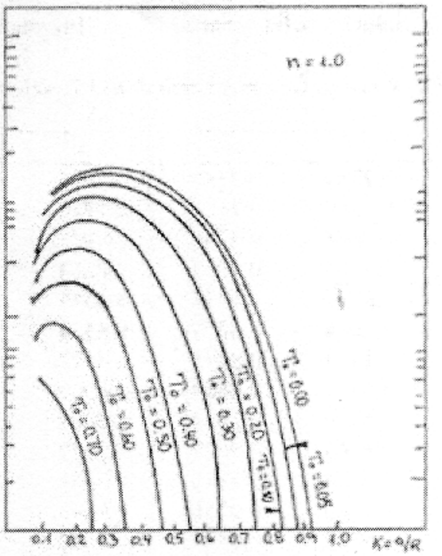


Figure 3. Dimensionless flow rate vs. dimensionless plunger radius for n = 1 (Osorio, 1985).

The dimensionless shear rate is obtained with $T_0$ value used in the following equation:

$$\left.\frac{d\phi}{d\rho}\right|_{\rho = K} = \left(\frac{\lambda(\lambda - T_0)^2}{K} - K - T_0\right)^{1/n} \tag{15}$$

And, the shear atress is obtained by replacing $P$ and $T_w$ into equation

$$\sigma = \frac{PRT_w}{2} \tag{16}$$

## 2. Materials and methods

The samples of caramel jam were taken from a Chilean market. It was packed in a cylindrical rigid plastic container with 3.24 ± 0.01 cm internal diameter and 4.10 ± 0.01 cm height.

2.1 Back extrusion test

Lloyd universal material testing (Lloyd Instruments Limited, Hampshire, England) machine model LR-5K was used to operate the plunger. The plunger was screwed to the crosshead of the Lloyd and a 500 N compression load cell was used.

The crosshead rate of the Lloyd testing machine varied from 2 mm/s to 600 mm/s.

The Lloyd testing machine was interfaced to a computer with a data analysis software (DAPMAT, version 3.05).

The plunger penetration was 70% of the sample height.

Soluble solid content was determined with a refractometer (Meichi Techno, Tokyo, Japan) model 58-92.

2.2 Sample

The samples were codified by soluble solid content and elaboration date.

All measurements were done at 20°C. The sample in the package was placed on the base plate, the plunger was in alignment with the cylinder containing the sample.

Table 2: λ values for the diferent $K$ and $T_o$ values for n=1

| $T_o/K$ | 0.1 | 0.2 | 0.3 | 0.4 | 0.5 | 0.6 | 0.7 | 0.8 | 0.9 |
|---|---|---|---|---|---|---|---|---|---|
| 0.05 | 0.7289 | 0.7389 | 0.7577 | 0.7818 | 0.8117 | 0.8466 | 0.8860 | 0.9292 | 0.9757 |
| 0.10 | 0.7469 | 0.7584 | 0.7770 | 0.8020 | 0.8328 | 0.8686 | 0.9088 | 0.9528 | - |
| 0.15 | 0.7648 | 0.7769 | 0.7963 | 0.8222 | 0.8539 | 0.8906 | 0.9316 | 0.9764 | - |
| 0.20 | 0.7825 | 0.7952 | 0.8154 | 0.8425 | 0.8749 | 0.9125 | 0.9544 | - | - |
| 0.25 | 0.8000 | 0.8134 | 0.8345 | 0.8622 | 0.8959 | 0.9344 | 0.9772 | - | - |
| 0.30 | 0.8174 | 0.8314 | 0.8534 | 0.8822 | 0.9168 | 0.9563 | - | - | - |
| 0.35 | 0.8345 | 0.8493 | 0.8722 | 0.9020 | 0.9377 | 0.9782 | - | - | - |
| 0.40 | 0.8513 | 0.8669 | 0.8909 | 0.9218 | 0.9585 | - | - | - | - |
| 0.45 | 0.8679 | 0.8844 | 0.9004 | 0.9415 | 0.9793 | - | - | - | - |
| 0.50 | 0.8843 | 0.9017 | 0.9279 | 0.9611 | - | - | - | - | - |
| 0.55 | 0.8924 | 0.9188 | 0.9461 | 0.9806 | - | - | - | - | - |
| 0.60 | 0.9160 | 0.9356 | 0.9643 | - | - | - | - | - | - |
| 0.65 | 0.9313 | 0.9521 | 0.9822 | - | - | - | - | - | - |
| 0.70 | 0.9461 | 0.9684 | - | - | - | - | - | - | - |
| 0.75 | 0.9605 | 0.9844 | - | - | - | - | - | - | - |
| 0.80 | 0.9744 | - | - | - | - | - | - | - | - |
| 0.85 | 0.9876 | - | - | - | - | - | - | - | - |

(Osorio, 1985)

$F_T$ was the recorded force just before the plunger was stopped and the $F_{Te}$ was the asymptotic recorded force after the plunger was stopped (See Fig.4).

The results were ordered by their soluble solid content.

Parameters for power law and Bingham plastic models were obtained with a spreadsheet, and statistics analyses were done with a statistical software (Statgraphics).

**3. Results and discussion**

Fig. 4 shows a typical diagram of force versus plunger position obtained from back extrusion testing. From this diagram, $F_{Te}$ value can be obtained when the system reaches equilibrium.

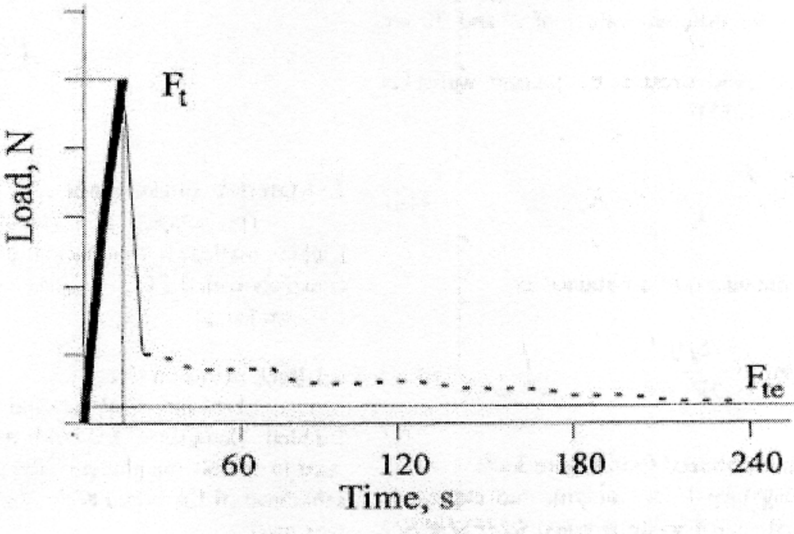


Figure 4. Typical force - displacement obtained from back extrusion of caramel jam.

3.1 Ostwald-de-Waele model

The flow behavior index was computed following the procedure outlined (Osorio and Steffe, 1987).

Table 3 shows different values of flow behavior index for different soluble solid content.

Table 3. Flow behavior index (power law model) for different soluble solid content of caramel jam.

| Soluble solid (%) | $n_{95\%}$ | $r^2$ |
|---|---|---|
| 71 | $0.34 \pm 0.17$ | 0.6640 |
| 72 | $0.75 \pm 0.02$ | 0.9983 |
| 73 | $0.69 \pm 0.10$ | 0.7721 |
| 74 | $0.71 \pm 0.08$ | 0.8908 |
| 75 | $0.18 \pm 0.02$ | 0.9525 |

For the different cases, the flow behavior index was lower than 1, this corresponds to a pseudo plastic fluid where apparent viscosity decreases with increasing shear (Skelland, 1967).

For 71% and 73% soluble solid, the value of power law model did not represent the experimental data.

Remember that the flow behavior index is the slope of a log - log plot of $(F_{cb2}/F_{cb1})$ $(L_1/L_2)$ against $(V_{p2}/V_{p1})$ with the $r^2$ value for the linear adjustment.

Table 4 shows the equations obtained fitting the power law models to different $\sigma$ and $\dot{\gamma}$ values obtained from the different soluble solid contents.

Table 4. Power law equation for different solid soluble content of caramel jam.

| Soluble solid (%) | Equation | $r^2$ |
|---|---|---|
| 72 | $\sigma = 1873\dot{\gamma}^{0.40}$ | 0.8984 |
| 73 | $\sigma = 1598\dot{\gamma}^{0.71}$ | 0.9227 |
| 74 | $\sigma = 2159\dot{\gamma}^{0.58}$ | 0.8688 |
| 75 | $\sigma = 2574\dot{\gamma}^{0.11}$ | 0.2085 |

The power law model best represent the flow behavior when the soluble solid content varied from 72% to 74%.

3.2 Bingham plastic model

Table 5 shows the equations obtained when fitting the Bingham plastic model for different soluble solid content.

Table 5. Bingham plastic equation for different soluble solid content of caramel jam.

| Soluble solid (%) | Equation | $r^2$ |
|---|---|---|
| 71 | $\sigma = 447 + 757\dot{\gamma}$ | 0.8362 |
| 72 | $\sigma = 330 + 1422\dot{\gamma}$ | 0.9218 |
| 73 | $\sigma = 800 + 1116\dot{\gamma}$ | 0.8471 |
| 74 | $\sigma = 1011 + 1421\dot{\gamma}$ | 0.8722 |
| 75 | $\sigma = 1024 + 1268\dot{\gamma}$ | 0.8395 |
| 76 | $\sigma = 1024 + 1268\dot{\gamma}$ | 0.8848 |

Bingham plastic model best represented caramel jam flow behavior for different soluble solid content and shear rate without the problem that represents the obtainment of n value for the power law model. ($\dot{\gamma} = 0.5 - 2.6 s^{-1}$)

3.3 Herschel - Bulkley model

This model did not represent the experimental value. (e.g. $r^2 = 0.58$)

3.4 Yield stress

Yield stress (Bingham model) increased as soluble solid content increased, with shear rate varying from 0.5 to 2.6 $s^{-1}$ (Fig. 5). This was also observed in tomato purees (Alviar and Reid, 1990), and grape juice (Rojo *et al.*, 1994).

Table 6 shows different equations applied to model yield stress dependence with soluble solid content.

Table 6. Equations applied to model yield stress dependence with soluble solid content.

| Equation | $r^2$ |
|---|---|
| $\sigma_0 = 8.9 \cdot 10^{-29}\, C^{16.4}$ | 0.9466 |
| $\sigma_0 = e^{(-10.8 + 0.23C)}$ | 0.9441 |
| $\sigma_0 = -1059.6 + (0.85C - 29.3)^2$ | 0.9403 |
| $\sigma_0 = -2085.7 + 0.65C^2$ | 0.9357 |
| $\sigma_0 = -3679.7 + (18.9C)^{1.2}$ | 0.9351 |
| $\sigma_0 = -4266.2 + 63.1C$ | 0.9345 |

Based on the coefficient of determination, the model that best represents caramel jam behavior is:

$$\sigma_0 = 8.9 \cdot 10^{-29}\, C^{16.4} \qquad (17)$$

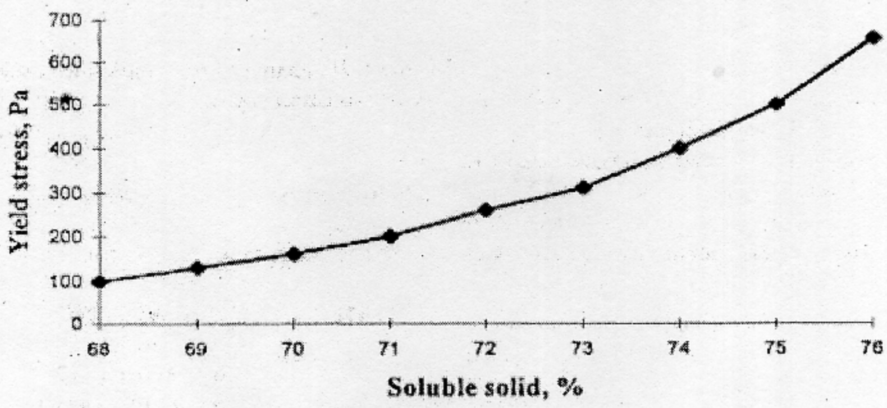


Figure 5. Yield stress vs. soluble solid content in caramel jam samples.

## 4. Conclusions

It is possible to describe the flow behavior of caramel jam using the back extrusion technique.

Bingham plastic model best described the flow behavior of caramel jam.

Soluble solid content has a strong influence on plastic viscosity, consistency coefficient and yield stress values.

## Acknowledgment

The authors would like to thank the financial support of Fondecyt (Project 1960403).

## 5. Nomenclature

$a$ : radius of the plunger, m

$\overline{AO}$ : level of fluid measured from the fluid surface to O, m

C : soluble solid content, %

$d$ : fluid density, $kg / m^3$

F : force applied to the plunger, N

$F_b$ : buoyancy force, N

$F_{cb}$ : force corrected for buoyancy, N

$F_T$ : recorded force just before the plunger is stopped, N

$F_{T*}$ : recorded force after the plunger is stopped, N

$g$ : gravity acceleration, $m/s^2$

$K$ : ratio of radius of plunger to that of outer cylinder, dimensionless = $a/R$

$L$ : length of annular region = $\overline{AO}+\overline{OB}$, m

$n$ : flow behavior index dimensionless

$n_{95\%}$ : flow behavior index dimensionless 95%

O : initial level of fluid when the plunger has not been forced down in the sample, m

$\overline{OB}$ : position of the plunger bottom, measured with respect to O, m

$P$ : pressure drop per unit of length, Pa/m

r : radial coordinate measured from common axis of cylinders forming annulus, m

$r^2$ : coefficient of determination

$R$ : radius of outer cylinder of annulus, m

$T$ : time, s

$T_o$ : yield stress, dimensionless

$T_w$ : shear stress at the plunger wall, dimensionless

$V_p$ : velocity of the plunger, m/s

$\dot{\gamma}$ : shear rate, $s^{-1}$

$\eta_{np}$ : plastic viscosity

$\lambda$ : value of dimensionless radial coordinate for which shear stress is zero

$\rho$ : radial coordinate = $r/R$, dimensionless

$\sigma$ : shear stress, Pa

$\sigma_0$ : yield stress, Pa

$\Phi$ : flow rate, dimensionless

## References


Alviar M. and D. Reid, "Determination of rheological behavior of tomato concentrates using back extrusion", *Journal of Food Science* 55, (2), 554-555 (1990).

deMan J., P. Voisey, V. Rasper and D. Stanley, *Rheology and Texture in Food Quality*, The AVI Publishing Company, INC., Westport, Connecticut (1976).

Osorio F. A., "Back extrusion of Power law, Bingham Plastic and Herschel-Bulkley fluids". *Thesis for the Degree of M. S. Michigan State University*. Department of Food Sciencie and human Nutrition, Michigan, USA. (1985).

Osorio F. A. and J. F. Steffe, "Back extrusion of Power law fluids. Example problem". Paper N°85-6003, *American Society of Agricultural Engineers*, Michigan, USA. (1985).

Osorio F. A. and J. F. Steffe, "Back extrusion of Power law fluids". *Journal of Texture Studies* **18**: 43-63 (1987).

Rojo O., E. Castro, M. Miranda, E. Parra and A. Guarda, "Propiedades reológicas de jugo de uva (variedad Pais)". *Alimentos* 19 (4), 5-10 (1994).

Skelland, A. H. P., *Non-Newtonian Flow and Heat Transfer*, John Wiley and Sons, Inc., USA. (1967).